TAO, Vol. 11, No. 3, 555-566, September 2000

Some Seismological Aspects of the 1999 Chi-Chi Earthquake in Taiwan

Tzay-Chyn Shin[1, *]

(Manuscript received 24 November 1999, in final form 13 February 2000)

ABSTRACT

The Chi-Chi earthquake is the largest inland earthquake in Taiwan during the 20th century. It caused severe damage in central Taiwan. Three possible induced earthquakes triggered by a mainshock are being examined from the strong ground motion data. The occurrence of these three-triggered events can be used to explain the difference between preliminary isoseismal map, based on the real-time data, and final one. They can also explain why a wide area of aftershock distribution was observed. On the other hand, the overshooting of ground motion at those stations located near the northern end of Chelungpu fault is probably the reason for the complex surface rupture observed between FengYuan and TungShih.

(Key words: Chi-Chi earthquake, Seismological aspects)

1. INTRODUCTION

On September 21, 1999, at 1:47 AM local time (17:47 Sep. 20 UT), an earthquake of magnitude M_L=7.3 took placed in central Taiwan. The epicenter is located near the town of Chi-Chi, from which the event was named. This event is the largest earthquake on the island in the past hundred years. The Central Weather Bureau (CWB) located the epicenter at 120.82°E, 23.85°N with a focal depth of 1 km which was initially determined by an automatic process. The focal depth was later refined to 8.0 km after more data became available. As of October 13, 1999, the officially released casualty figures were 2333 dead, 10,002 injured, with more than 100,000 houses destroyed. About 80 km of rupture was observed along the Chelungpu fault with the largest measured vertical offset reaching more than 5 meters.

The purpose of this article is to discuss some seismological aspects of the Chi-Chi earthquake sequence and to present the strong motion data recorded by accelerographs which were installed under the Taiwan Strong-Motion Instrument Program (TSMIP) between 1992 and 1997, a network that covers the entire island.

[1]Central Weather Bureau, Taipei, Taiwan, ROC

*Corresponding author address: Dr. Tzay-Chyn Shin, Central Weather Bureau, 64 Kung-Yuan Road, Taipei, Taiwan, ROC; E-mail: shin@taiwan.cwb.gov.tw

2. HISTORICAL SEISMICITY AND LOCAL GEOLOGICAL SETTINGS

The Philippine sea plate and Eurasian plate collide with each other with the suture zone located along the Longitudinal Valley and give rise to a very complex structure in the Taiwan area. The seismicity and tectonics of eastern Taiwan are interesting simply because of the nature of the tectonic processes associated with the plate subduction and plate collision. With regard to damage, the historical records show that moderate to large earthquakes in western Taiwan have caused severe damages because they are shallow and occurred along active faults that are very close to the heavily populated areas. The Chi-Chi earthquake is a remarkable example. Figure 1 shows the locations of earthquakes with magnitude greater than 6.0 occurring in the Taiwan area, as obtained from the CWB's Seismology Center catalog from 1900 to 1999. The solid asterisks are the earthquakes after 21 Sep., 1999 and the solid circles are those before the Chi-Chi earthquakes. It is recognized historically in the Chi-Chi area where only two earthquakes with magnitude 7.1 were located. The Chi-Chi earthquake occurred in a region only with relatively low recent seismicity as comparing to the southwest of Taiwan prior to the earthquake.

In the west-central part of Taiwan, where the Chi-Chi earthquake occurred, there are at least three major Quaternary faults -- the ShuangTung fault, the Chelungpu fault and the ChangHua fault -- from east to west, respectively, and striking nearly north-south with an eastward dip. The ShuangTung fault is thrusting over the Quaternary Toukoshan Formation and the Chelungpu fault is thrusting over the younger alluvium deposits of the TaiChung basin. The hanging wall of the Chelungpu fault is mainly composed of the Chinshiu shale or the Kueichulin Formation. The Chelungpu fault is thuscategorized as the major geological structure in this area. The ChangHua fault is the frontal thrust fault in the west and is partially covered by recent alluvium deposits.

3. MODERN SEISMIC MONITORING

At the beginning of 1990, the CWB began to install a new seismic network (CWBSN) which eventually included 73 stations in the Taiwan area (Fig. 2). Digital telemetry and digital recording of conventional three-component short-period velocity sensors were used for seismic monitoring operation. In 1992, the CWBSN added three-component high-quality force balanced accelerometers to all CWBSN stations, and these are shown as asterisks following the station codes in Fig. 2. Their signals are also simultaneously digitally telemetered in real-time to the CWB headquarters in Taipei. The new system is called as RTD, and with maximum $\pm$ 2g capacity, has been used for the real-time recording and processing operation. Also, an effort to develop a Taiwan Rapid Earthquake Information Release System (TREIRS) has been successfully accomplished (Lee and Shin 1997; Teng et al. 1997; Wu et al. 1997). Currently, the system can routinely release the location and magnitude of a strong earthquake, as well as the intensity distribution, about 60 seconds after the occurrence of an inland earthquake. This capability makes Taiwan one of the leaders in rapid earthquake response around the world.

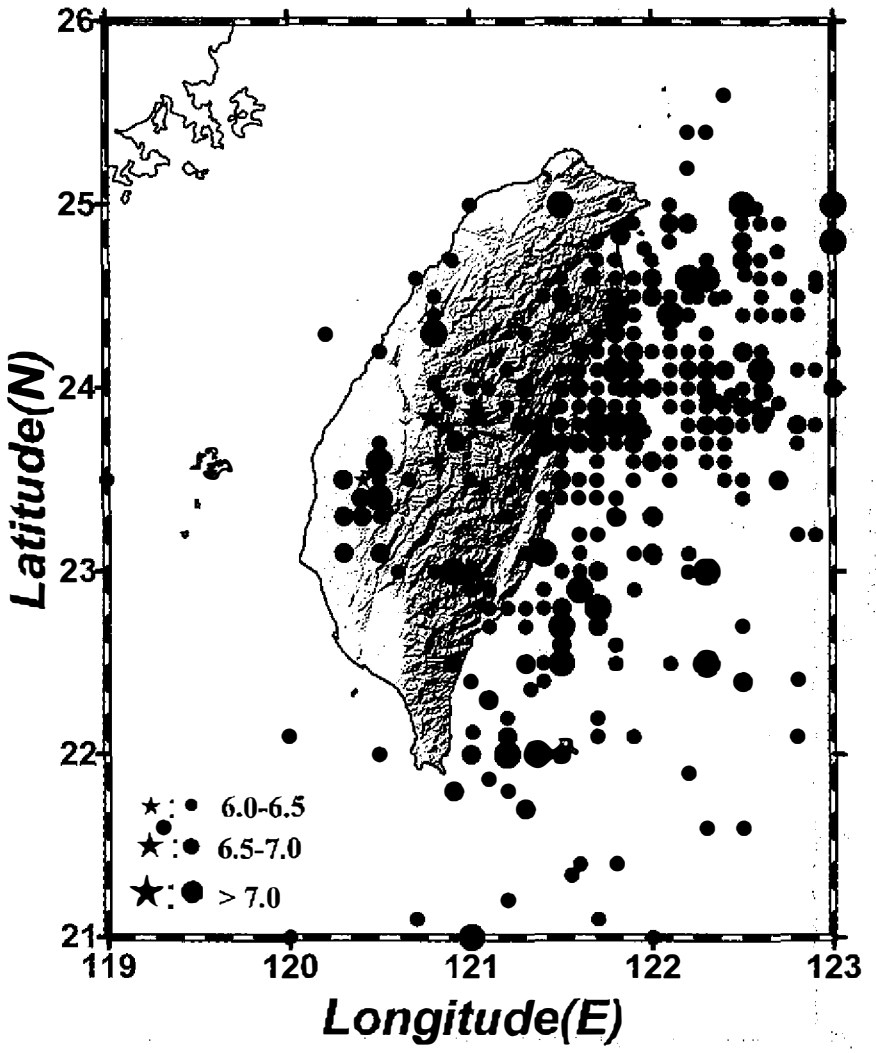

Fig. 1. Historical earthquakes with magnitude greater than 6 during 1900-1999. The solid circles represent the event occurring before the 21 September, 1999.

4. MAINSHOCK

Information on the Chi-Chi mainshock including the origin time, location, and magnitude were determined within 2 minutes (exactly 102 seconds) and immediately released through TREIRS. The CWB has also used near real-time digital acceleration data and a PGA attenuation curve (Shin 1998) to generate an isoseismal map (with CWB intensity scale) 3 minutes after the occurrence of the mainshock. The largest intensity VI(>250 gal) areas, which included the Counties of TaiChung, ChangHua, NanTou, YunLin, and ChiaYi, were defined

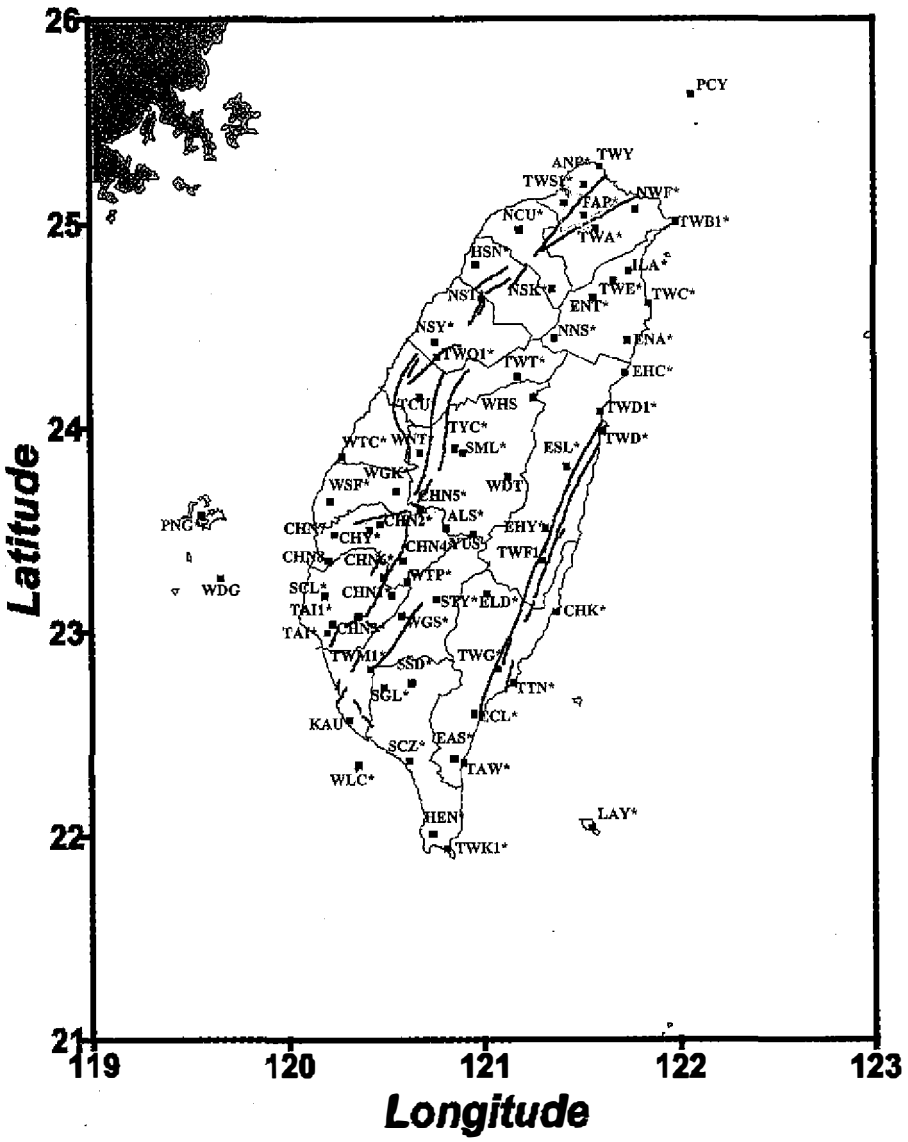

Fig. 2. Station distribution of CWBSN. The 73 stations are all equipped with three component velocity sensors. The 63 stations with asterisks following the station codes also having real-time acceleration digital output for seismic monitoring.

initially as potentially heavy damage areas. It turns out that the estimation was fairly accurate. Figure 3 shows the comparison of the isoseismal map issued preliminarily and the final one which was revised about one month later following collection of all the observed strong motion data. It is worth noticing that the area of intensity VI elongated toward north and south.

On examining the strong motion data at these two tip areas, we have found that at least three induced earthquakes occurred within one minute after the mainshock. The signals from the induced event are mixed with the mainshock signal. They can hardly be distinguished from one and another to be used to determine their location and magnitude (Fig. 4). The bottom-left trace is the vertical strong motion data at station CHY080 at about 32 km south of mainshock. The two sets of P and S wave arrivals can be clearly distinguished. The bottom-right traces are from station CHY028 at about the same epicenter distance but northwest of CHY080. The tail parts of the seismogram are a scramble of all other event signals together. It is very difficult to separate two sets of P and S wave arrival. The top-left traces belong to station TCU095 at 94 km north of the mainshock, the signal indicated by an arrow is definitely from another very close event judging from the very short ts to tp time. The other three closing stations TCU045, NST and TCU047 have recorded the similar signals. Using ts-tp time difference and the local PGA distribution, two induced events in the south part were approximately located at 120.66°E, 23.61°N and 120.78°E, 23.45°N while magnitudes were roughly estimated around to be 6.0-6.5. These two induced earthquakes may explain the geological failures, such as landslides and liquefaction that occurred in neighboring areas. Location of one induced event that oc-

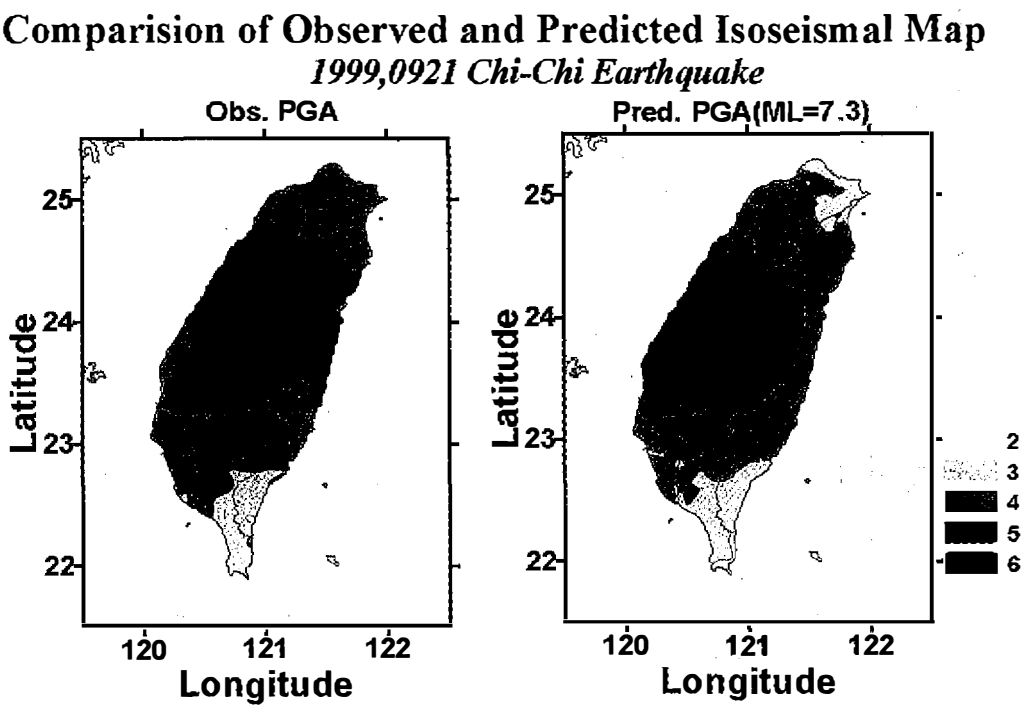

Fig. 3. Comparison of observed and predicted isoseismal maps. Predicted isoseismal map issued three minutes after the occurrence of the mainshock was constructed using real-time acceleration data and attenuation curve (Shin 1998). The observed isoseismal map was plotted after collection of all strong motion data. The differences are discussed in the text.

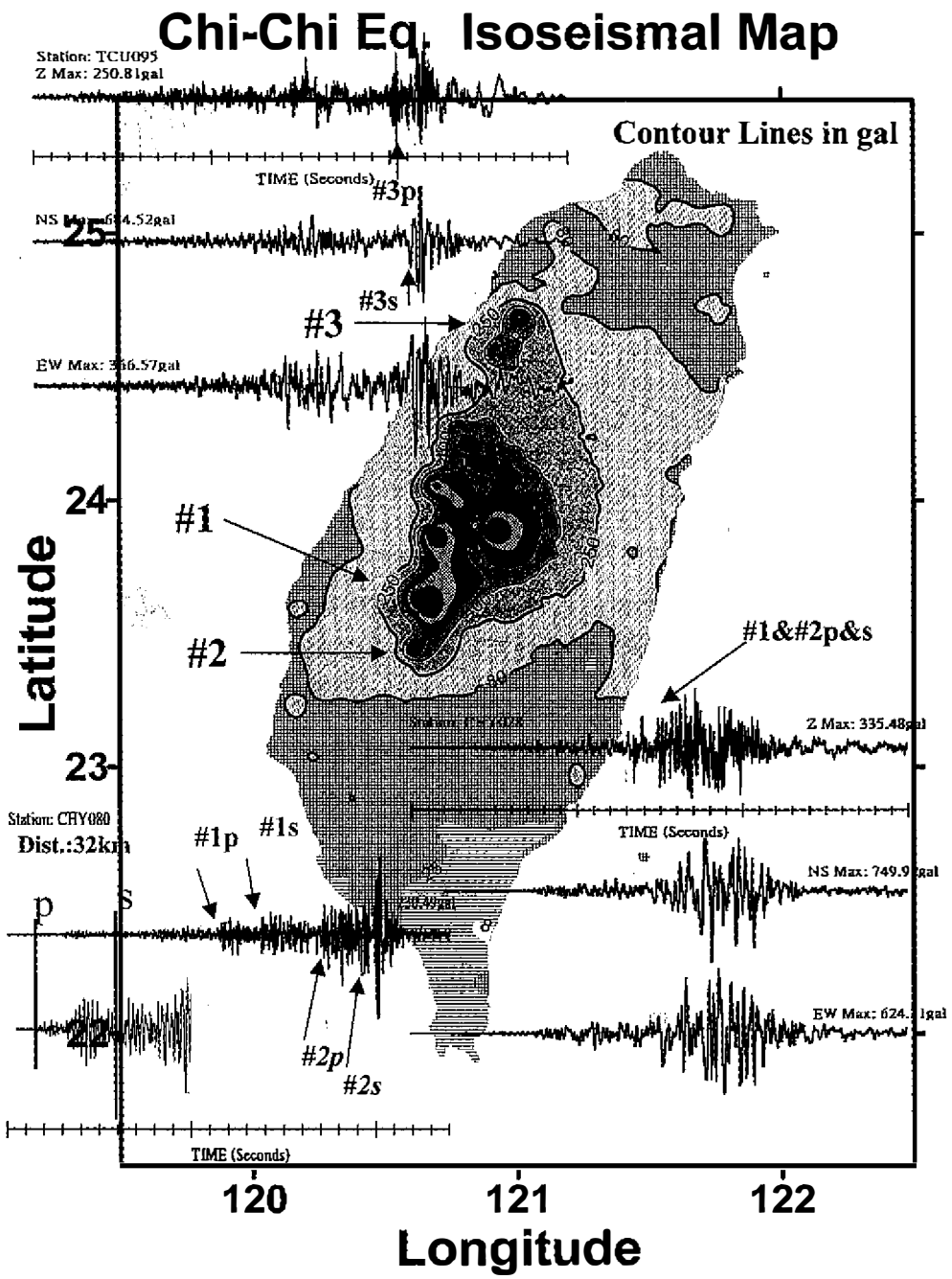

Fig. 4. The evidences from the three induced earthquakes are examined graphically. The event is marked with # symbol. The three sets of P and S wave arrivals are indicated as arrows. The detailed information from these three triggered events are discussed in the text.

curred in the northern part was placed at 121.01°E; 24.69°N and the magnitude was given as around 6.0. These magnitudes were estimated by comparing the peak ground motion with similar shallow event that occurred at a similar distance in the past. The occurrence of these three induced events can explain the difference between isoseismal maps, and the distribution of aftershocks as well. In addition, the peak ground acceleration recorded by the stations located in the area of the induced earthquakes is shown on the NS component while most of other stations have recorded the peak ground on the EW component. It turns out that the mechanisms of the induced earthquakes are different from that of the Chi-Chi earthquake.

Combining the first motion polarity of short-period seismograms and strong motion data, the focal mechanism of the mainshock shows two almost north-south striking planes. The east-dipping plane, with dip 30°, strike N20°E, and rake 85° , is consistent with the geologically observed rupture outcrop and aftershock distribution of the area.

5. AFTERSHOCKS

The felt event, including aftershocks of the Chi-Chi earthquake, and the locations as determined by the RTD system, are shown in Fig. 5. The aftershocks of the Chi-Chi earthquake were distributed over an area of about 40 by 100 square kilometers. Most of the aftershocks occurred on the eastern side of the Chelungpu fault because the fault is an east-dipping thrust fault. It is interesting to observe that the aftershocks disappeared on the eastern side against the Central Mountain Range (CMR). The three aftershocks with magnitude greater than 6.5 are all located in this area, while some smaller aftershocks occurred on the other side of the CMR. It appears that the ductile material beneath the CMR plays a very important role in preventing the occurrence of earthquake, but it can transfer released energy from one side to the other. The earthquakes at the northern and southern ends of the aftershock distribution area are due to the induced earthquakes. These events should be treated as individual earthquake sequences. In addition, a clustering distribution in ChiaYi county is the location of the 22 October, 1999 ChiaYi earthquake.

6. STRONG GROUND MOTION DATA

The strong motion data recorded at many stand-alone stations in the source region were collected during the two weeks following the mainshock. Figure 6 presents two sets of acceleration data recorded at station TCU129 and TCU089. They show the highest acceleration above 1G for the EW components. At station TCU089, the relatively low frequency signal shown for horizontal components may be associated with the site characteristics at TCU089, which is located on the slope of a hill. Figure 3 shows that the contours of the strong ground shaking appear to elongate along the fault line and the ground motion on the hanging wall side is stronger than that on the side at the foot of the wall. This agrees with the distribution of severely damaged areas. The result is also consistent with the focal mechanisms determined from the first motion solution as well as from the field investigation of the Chelungpu fault.

The displacement of ground motion can be obtained directly from a double integration of

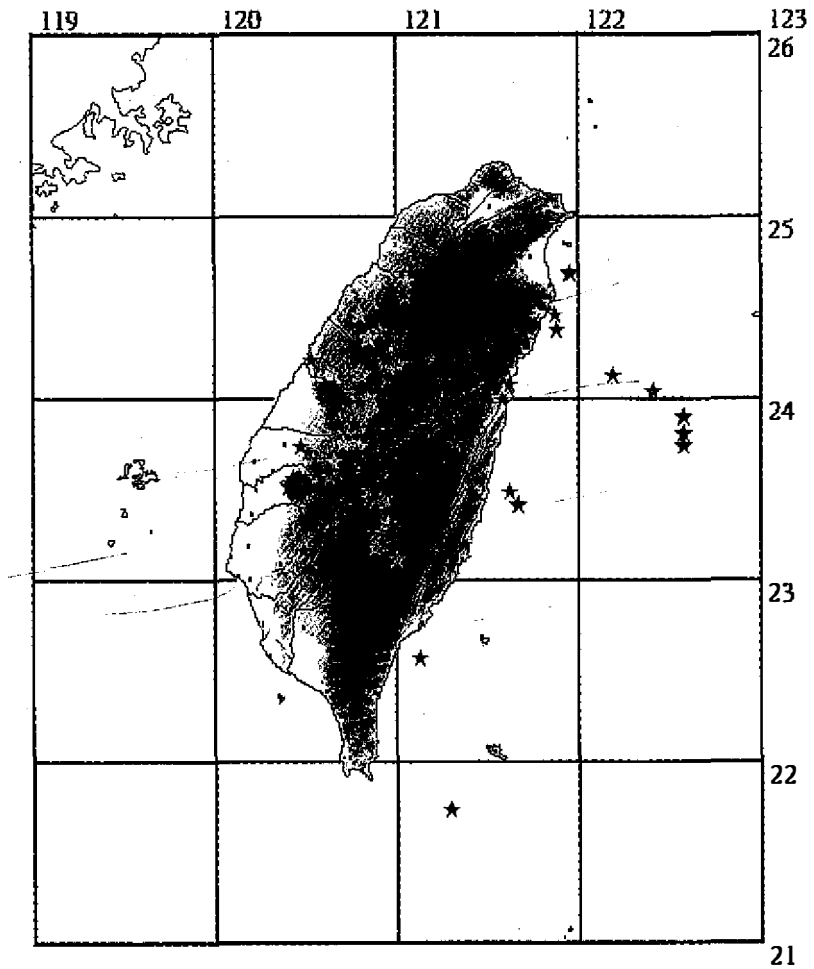

Fig. 5. The distribution map of felt events after the Chi-Chi earthquake. The earthquakes including the aftershocks of the Chi-Chi mainshock are those only triggered by RTD system. A clustering distribution in ChiaYi County is the place where the 22 October, 1999 ChiaYi earthquake occurred.

the acceleration data, while only the long-term trend removed. Figure 7 (Chung and Shin 1999) presents an example of data processes for station TCU068 located at the northern end of the Chelungpu fault. The three sets of traces represent acceleration, velocity and displacement, respectively. The permanent offset of displacement can be clearly observed in the source region, especially along the fault line. The distribution of permanent displacement in Fig. 8 derived from strong ground motion data is consistent with the deformation derived from the satellite image map. It appears that the thrust fault is mainly moving westward at the southern end of the Chelungpu fault with increased movement to the northern end where the thrust becomes an oblique faulting with increasing strike-slip component. The direction of move-

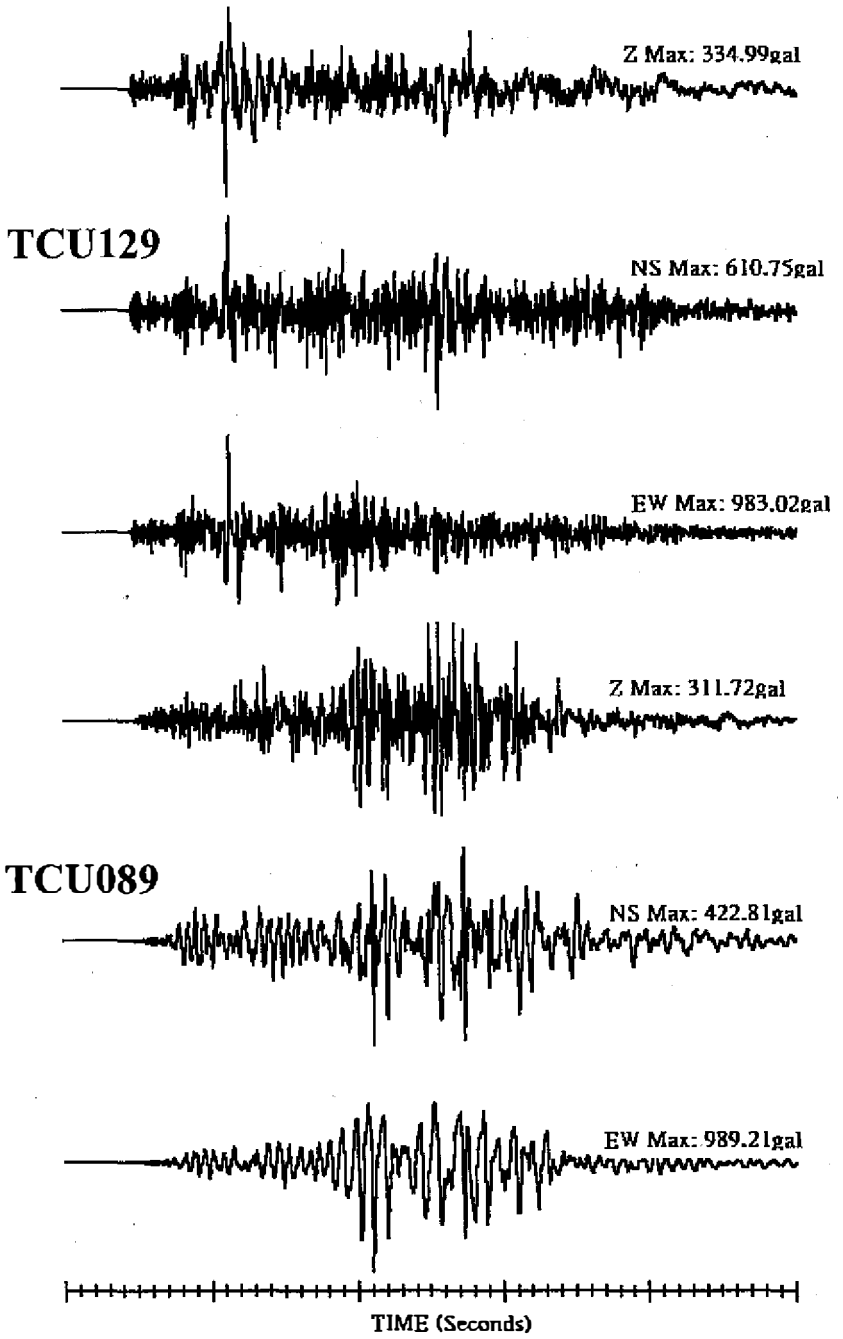

Fig. 6. Two sets of strong ground motion data. They both show the highest acceleration above 1G for the EW components. The horizontal components of the TCU089 acceleration records show relatively low frequency due to the site effects.

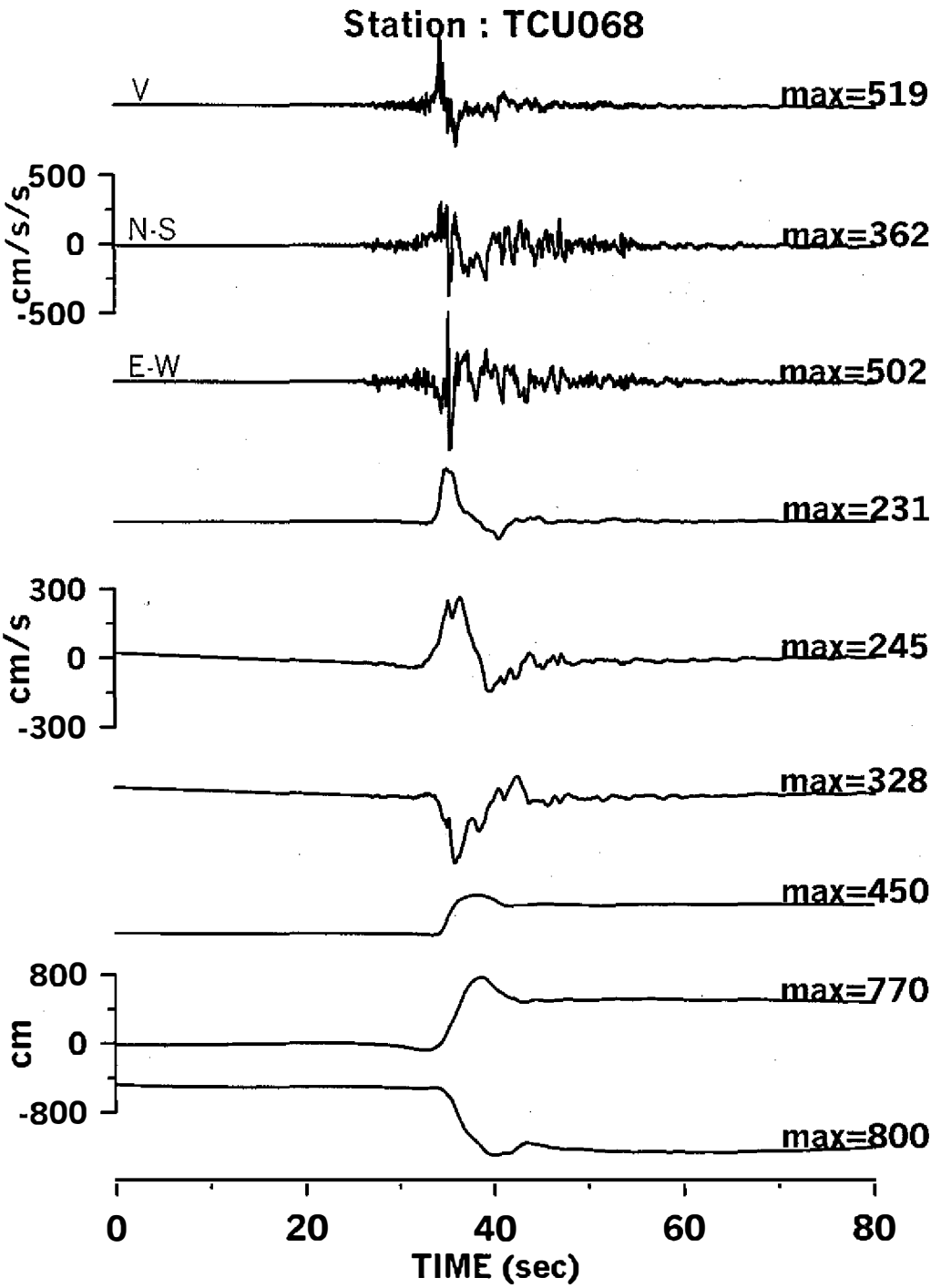

Fig. 7. Example of data processing. The acceleration records for station TCU068 are integrated to velocity and displacement shown from up to down.

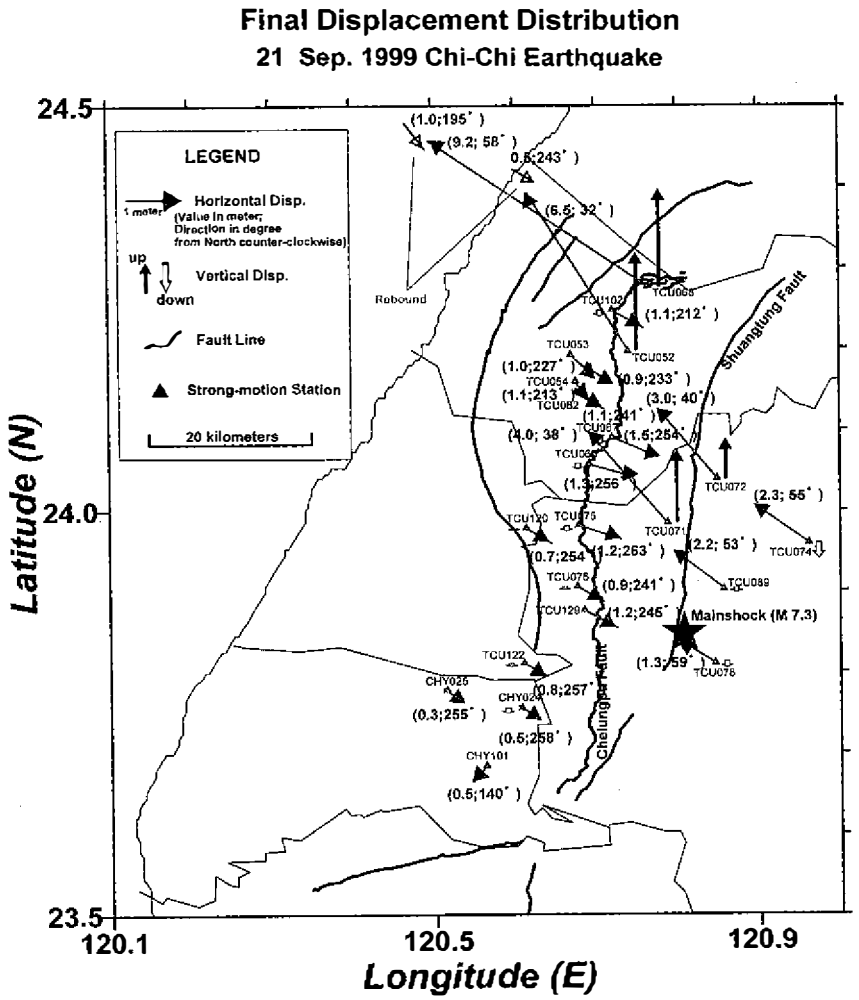

Fig. 8. Vectorized final displacement distribution. In general, the final displacement distribution is consistent with the satellite images and field investigations. The values appeared in the parentheses are horizontal displacement and its direction is counter clockwise from north. The rebound displacement and direction for two stations at the northern end of Chelungpu fault are also shown.

ment is gradually turning from east-west to north-west northward along the fault. In addition, the uplift in the hanging wall decreases eastward away from the fault line and becomes a subsidence in the Puli area. The relatively small southeastward movements and subsidence are also observed on the foot wall side. The hanging wall exhibits larger ground movement than those on the foot wall side. The displacement signal at TCU068 integrated directly from acceleration shows the offset increasing to about 9.2 meters northwestward with a 1 meter over-

shoot before returning to its final state. The similar phenomena, indicated by rebound arrows in Fig. 8, can be found in stations at the northern end of the fault.

8. CONCLUSIONS

1. The TREIRS of the CWB is capable of performing rapid earthquake reports for inland earthquakes in about one to three minutes. The information includes origin time, location and depth, as well as isoseismal mapping. Taiwan currently leads the world in the accomplishment rapid earthquake reporting which will ultimately be evolved toward an early warning system for significant earthquakes. The CWB target is trying to provide a 5-10 second warning time before the strong-shaking arrival of large events from the east coast.
2. The ruptural processes of mainshock are more complicated than expected. According to the analysis of strong motion data under TSMIP, at least three induced earthquakes were triggered within one minute of the mainshock. The induced events can explain the wide distribution of aftershocks.
3. The final displacements derived from strong motion data show good agreement with the results of fault rupture from field investigation. The overshoot shown at the northern end of the Chelungpu fault might explain the complex surface rupture observed between FengYuan and TungShih where some back-thrust ground failures were seen.

Acknowledgments The author wish to express his appreciation to the Central Weather Bureau for their kindness in providing data used in this study, especially to Dr. J.K. Chung for help with the permanent displacement calculation. Comments from Dr. Leong Teng and Dr. Francis Wu. are gratefully acknowledged

REFERENCES

Chung, J. K., and T. C. Shin, 1999: Implications of rupture processes from the displacement distribution of strong ground motions recorded during the 21 September Chi-Chi, Taiwan earthquake. *TAO*, **10**, 777-786.

Lee, W. H. K., and T. C. Shin, 1997: Realtime seismic monitoring of buildings and bridges in Taiwan, in "Structural Health Monitoring. In: F. K. Chang (Ed.), 777-787, Technomic Pub. Co, Lancaster, PA.

Shin, T. C., 1998: A preliminary study of the earthquake early warning system in the Taiwan area. *Metor. Bull.* **42**, 118-134. (in Chinese).

Teng, T. L., Y. M. Wu, T. C. Shin, Y. B. Tsai, and W. H. K. Lee, 1997: One minute after: strong motion map, effective epicenter, and effective magnitude. *Bull. Seism. Soc. Am.*, **87**, 1209-1219.

Wu, Y. M., T. C. Shin, C. C. Chen, Y.B. Tsai, W. H. K. Lee, and T. L. Teng, 1997: Taiwan rapid earthquake information release system. *Seism. Res. Letters*, **68**, 931-943.